coatings

MDPI

Review

Microstructure and Performance of High-Velocity Oxygen-Fuel Coupled Physical Vapor Deposition (HVOF-PVD) Duplex Protective Coatings: A Review

Yingpeng Zhang [1,2], Qun Wang [3], Chidambaram Seshadri Ramachandran [4], Peng Guo [1,2] and Aiying Wang [1,2,*]

[1] Key Laboratory of Marine Materials and Related Technologies, Zhejiang Key Laboratory of Marine Materials and Protective Technologies, Ningbo Institute of Materials Technology and Engineering, Chinese Academy of Sciences, Ningbo 315201, China
[2] University of Chinese Academy of Sciences, Beijing 100049, China
[3] College of Materials Science and Engineering, Hunan University, Changsha 410082, China
[4] Department of Materials Science and Engineering, The State University of New York at Stony Brook, New York, NY 11794, USA
* Correspondence: aywang@nimte.ac.cn

Abstract: The paper summarizes the current development of high-velocity oxygen–fuel coupled physical vapor deposition (HVOF-PVD) duplex coatings as protective candidates. Following a detailed historical overview of HVOF and PVD technologies, the fabrication methods for duplex protective coatings are presented. The duplex coating superimposes the synergistic advantages of coatings deposited by HVOF and PVD, where the traditional weaknesses of each technique are modified to a great certain extent. Subsequently, the relation between structural characteristics of the duplex coatings and their mechanical, tribological, and corrosive behavior is described in detail. It is demonstrated that the duplex coatings show more excellent overall performance than coatings deposited by both HVOF and PVD separately. Finally, we summarize the protective performance and promising potential of HVOF-PVD duplex coating for applications as well as the research prospects of challenges in future.

Keywords: thermal spray; HVOF; PVD; microstructure; mechanical properties; wear; corrosion; surface engineering

Citation: Zhang, Y.; Wang, Q.; Ramachandran, C.S.; Guo, P.; Wang, A. Microstructure and Performance of High-Velocity Oxygen-Fuel Coupled Physical Vapor Deposition (HVOF-PVD) Duplex Protective Coatings: A Review. *Coatings* **2022**, *12*, 1395. https://doi.org/10.3390/coatings12101395

Academic Editor: Matjaž Finšgar

Received: 2 September 2022
Accepted: 21 September 2022
Published: 24 September 2022

1. Introduction

Thermal spraying is a general term for a series of coating processes. The process involves the powder material being given thermal and kinetic energy in a hot air flow medium and sprayed onto the substrate at high speed to form a coating [1–4]. Over the past few decades, a series of thermal spray technologies have been developed, such as electric arc spraying (EAS), plasma spraying (PS), detonation spraying (DS), and high-speed oxy-fuel (HVOF) spraying [5–9]. In particular, HVOF spraying achieves a favorable combination of thermal and kinetic energy due to its high speed (~1500 m/s) and relatively low temperature (~2000 °C) [10]. In addition, it benefits the advantage of high flexibility (such as the deposition of cermets, oxide and oxide-free ceramics coatings) and low cost for mass production [11,12]. Thus, HVOF coating as a protective candidate has been widely used in various industrial fields, such as aviation, aerospace, petroleum, and marine components as well as systems [13–15]. The process of preparing the coating by HVOF spraying is shown in Figure 1. [16,17]. It can be observed that the raw material powder and the spraying process are two key factors for the coatings prepared by HVOF spraying. Therefore, designing and optimizing the raw material powder and spraying process parameters is quite crucial before coating deposition. Typically, the powder material consists of a

metal/ceramic primary phase and metal binder phase (Co, Cr, Ni, etc.) with a particle size distribution of 10–40 μm [18–20]. At present, a variety of commercial feedstock powders have been developed, mainly including but not limited to WC-based, Cr_3C_2-based, and Fe-based powders [21–23]. Moreover, many researchers have conducted structural and compositional modifications based on commercial feedstock powders to obtain high-quality HVOF spray coatings [24–26]. In addition, the HVOF spraying parameters particularly involving the feature and flow rate of working gas and the ratio of oxygen/fuel gas make a great contribution to the temperature, airflow velocity and decomposed composition during deposition, which could change the structure and properties of coatings, such as strength, toughness and residual stresses, to a great extent [10,27]. As a result, it is empirically known that the performance of HVOF spray coating shows strong dependence upon the combined effect of feedstock powder materials and the spraying processes.

Differently, with the thermal spraying, the physical vapor deposition (PVD) process has been around for over 100 years, and the specific "physical vapor deposition" was not named until the 1960s [28]. However, with the development of plasma physics in modern industry, the vacuum-coating process based on plasma discharge has achieved revolutionary progress, which has derived various technologies, such as magnetron sputtering, thermal evaporation, and cathodic arc deposition [29–32]. Specifically, PVD technology refers to the physical method of vaporizing the material source (often called a target) surface into atoms, molecules, or ions under vacuum conditions and transporting them through a low-pressure gas (or plasma) to form a thin film on the substrate.

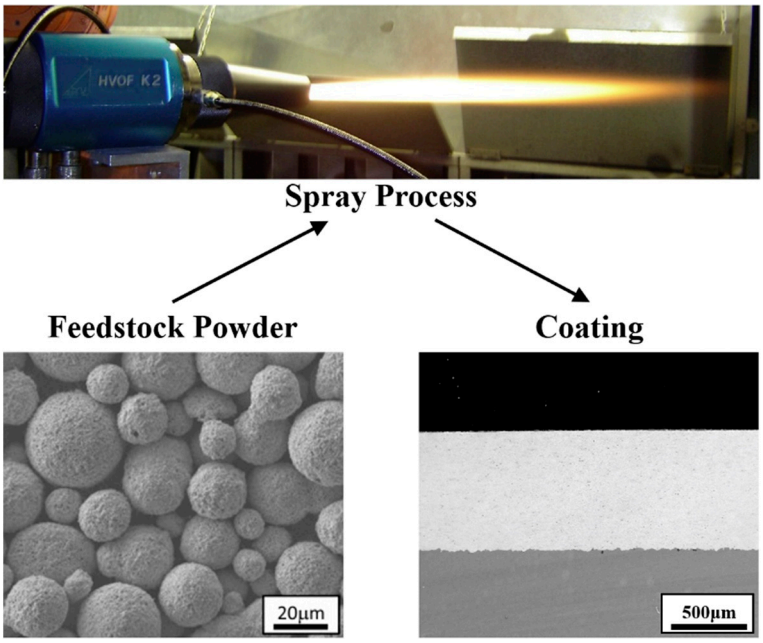

Figure 1. Schematic diagram of the coating prepared by HVOF spraying. Reprinted with permission from Ref. [16]. Copyright Elsevier, 2015. Reprinted with permission from Ref. [17]. Copyright Elsevier, 2019.

As an advanced surface treatment technology, the PVD deposition process can be divided into three stages: target vaporization, vapor phase transport, and thin film deposition. As shown in Figure 2, depending on the way the target is vaporized, PVD can be categorized into two main types of technologies: sputtering and evaporation [33]. During the sputtering process, a magnetic field is formed by an array of magnets located near the target. The gas enters the chamber and is ionized into positive ions, which are then attracted to the negatively charged cathode target and bombard the target in an accelerated manner. The bombarded target surface releases atomic scale particles, which are violently projected onto the substrate to form a thin film/coating [33–35]. In the evaporation process,

the cathode target serves as the source material. Through electron beam evaporation, multi-arc evaporation ionization, and other processes, the particles in the target are evaporated and ionized into positive ions and electrons [36–38]. It should be emphasized that a negative bias is usually applied to the substrate to attract positive ions. Subsequently, a film/coating is rapidly formed on the substrate. In a word, PVD technology has made significant progress to date, with deposit types focusing on carbon-based and nitrogen-based composite coatings [39–42].

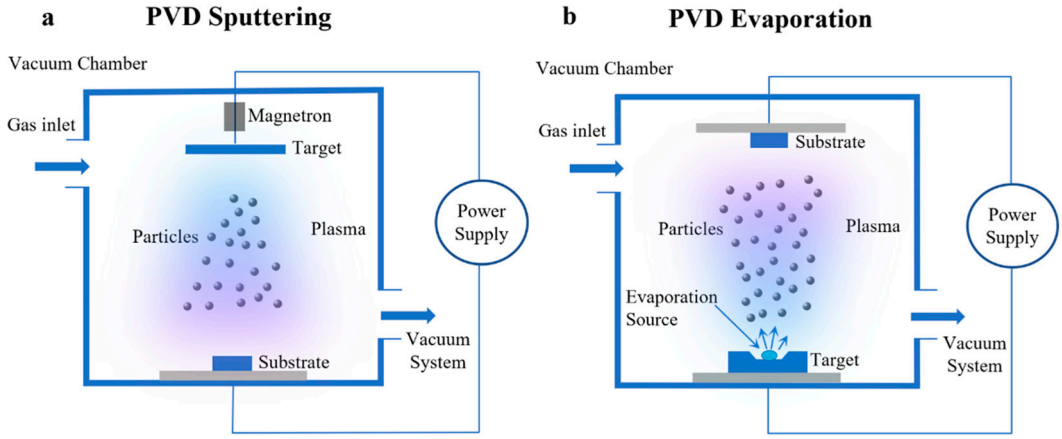

Figure 2. PVD deposition coating methods: (**a**) sputtering, (**b**) evaporation. Reprinted with permission from Ref. [33]. Copyright Elsevier, 2018.

As a "magic coat" of materials, protective coatings provide an effective guarantee for the long-term and stable service of key components in the engineering field. HVOF and PVD are two widely used surface modification techniques that prepare coatings with their demanded characteristics. For HVOF coatings, the deposition rate is very high, allowing thick and hard coatings to be produced in a short period. Moreover, relatively thick coatings are effective for protecting materials used in harsh environments. However, as a conventional wear-resistant coating, its performance in corrosive environments is unsatisfactory, because the intrinsic defects of thermal spraying, grain boundaries, porosity, and microcracks inside the deposit are detrimental to the corrosion resistance of HVOF coatings [17,43–45]. Different from the poor adhesion between coating with semi-molten droplets and substrates, PVD coatings are usually dense and corrosion resistant over large uniformity, especially self-lubricating and chemically inert carbon-based coatings/films [46,47]. However, due to the large internal stresses and poor toughness of thin PVD coatings caused by ion bombardment with high energy during deposition, the coatings suffer from the comprehensive properties of high hardness and weak adhesion to soft metallic substrates (refers to iron, steel and other low-hardness metal materials, especially light alloys, such as Mg, Al, and Ti). In particular, the substrate easily undergoes the serious plastic deformation under the heavy load conditions, which can thereafter lead to catastrophic delamination/flaking of the top PVD protective coating [48–50]. Many researchers have recently proposed a new "duplex coating" system based on HVOF and PVD [45,50–60].

The structure of duplex coating consists of a thick HVOF bottom layer and a thin PVD top layer, as shown in Figure 3. There are two distinctive features of this coating system: the first is a cumulative advantage. Duplex coatings incorporate the synergistic advantages of both coatings by each deposition technique, such as the excellent hardness and wear resistance of HVOF coatings and the good corrosion resistance of PVD coatings with a dense structure. The second is to make up for the disadvantage. The thick and hard HVOF coating acts as an intermediate layer, which provides effective support and a smooth transition between the soft substrate and the hard yet brittle PVD coating. It can largely avoid delamination and flaking of the PVD top layer due to the film-based

interface mismatch during the stress/friction process [61]. Meanwhile, the dense PVD top layer uniformly covers the HVOF coating with high porosity, which can improve the corrosion resistance of HVOF coating by sealing pores and reducing chemical activity [44,45]. It can be considered that the duplex coating is an ingenious "two birds with one stone" strategy.

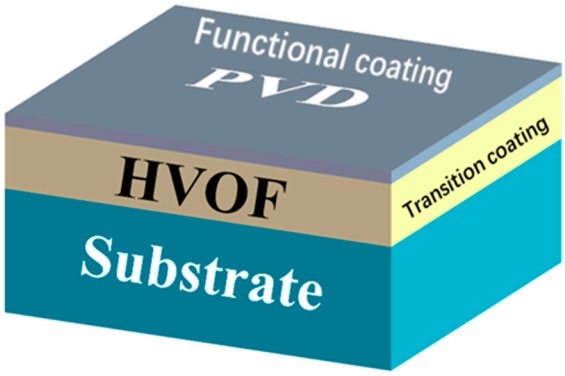

Figure 3. Structure of HVOF-PVD duplex coating.

In this review, the microstructure and properties of HVOF-PVD duplex coatings and their potential application in the field of surface protection are described and discussed in next three structured sections. Section 2 describes the surface and cross-sectional topographic characteristics of the deposited duplex coating. Section 3 reviews the properties of duplex coatings in detail, including mechanical properties, tribology, and corrosion behavior. Finally, Section 4 summarizes the protective performance and application potential of duplex coating, where the research prospects for future are proposed as well.

2. Microstructure and Morphology of Coatings

The microstructure of the coating is closely related to its protective capabilities, such as mechanics, wear, and corrosion resistance. Therefore, the morphology of the duplex coating (containing cross-section and surface) is of great concern. The morphology of the duplex coating is jointly determined by the HVOF and PVD coatings. It is worth noting that the thick HVOF bottom layered coating can be considered as a promising and yet tough substrate for the thin PVD top layered coating in these combined duplex coatings. During HVOF technology, the coatings with tens of micrometers thickness can be easily deposited to the pristine substrate due to the flattened molten particles with kinetic energies, which yield the protective performance of coating with high mechanical and tribological properties. However, note that the surface of HVOF coatings is rather rough with accumulated molten macro-particles. For PVD technology, even the deposited coatings with only several micrometers of thickness, the formed dense structure benefited the substrate candidates with superior mechanical, tribological and electrochemical properties. However, in order to prolong the performance of coatings in harsh conditions, it is necessary to apply the PVD coating as a top layer on the HVOF mechanical transition layer beyond the substrates, in which the pretreatment, including grinding, ultrasonic cleaning and ion etching, is pre-required to reduce the surface roughness and macroparticle defects of sublayered HVOF coatings and thereafter to obtain the superior combination of performance for HVOF-PVD duplex coatings. Picas et al. [50] prepared Cr_3C_2-NiCr/TiN (TiAlN) duplex coatings on light alloys by combining HVOF and PVD techniques. Figure 4a,b shows the cross-sectional images of the Cr_3C_2-NiCr/TiN and Cr_3C_2-NiCr/TiAlN duplex coatings, respectively. It can be seen that the HVOF coating consists of carbide and metal binder phases. The carbide grains dispersed in the binder phase were decomposed and

dissolved to some extent during the spraying process. Thus, as reported in their study, clearly visible pores and microcracks appeared inside the HVOF coating. In contrast, the PVD top layer exhibits a uniform single-phase microstructure. The interior is quite dense with no obvious pores. It is worth noting that the interface between the PVD top layer and the HVOF bottom layer is tightly bonded without visible defects. It implies a good interfacial adhesion between the two coatings. Moreover, the microstructure of HVOF coating is layered and wavy, while that of PVD coating is dense and uniform, which can perfectly complement each other. In addition, Tillmann et al. [62] investigated the effect of heating and etching pretreatment of HVOF coatings on the duplex coating. As shown in Figure 4c,d, they found that heating and etching could obtain a smoother HVOF (WC-Co) coating surface. Further, the defects at the interface of the WC-Co/CrAlN duplex coating were reduced, which resulted in a dense and uniform morphology of the PVD top layer. The surface SEM images of the PVD (CrN) coating, HVOF (Cr_3C_2-NiCr) coating, and HVOF-PVD (CrN/Cr_3C_2-NiCr) duplex coating are shown in Figure 5 [55]. It can be observed that the PVD coating surface is relatively flat in the three samples. However, due to the anti-sputtering effect of the PVD process [63,64], many smaller-sized particles and pits are still distributed on its surface. Unlike this, the HVOF coating surface exhibits a very large number of pores. This phenomenon is considered to be typical of the surface morphology of HVOF coatings [8,65].

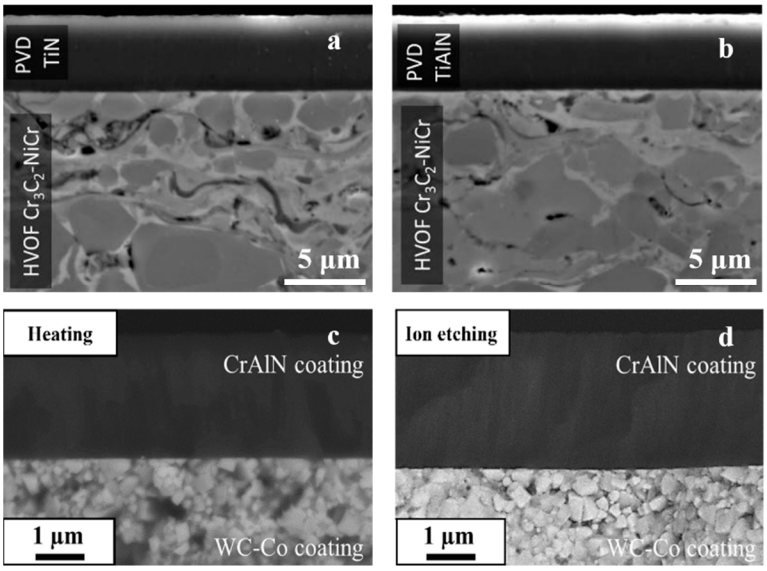

Figure 4. Cross-sectional microstructure of HVOF-PVD duplex coatings: the (**a**) Cr_3C_2-NiCr/TiN, (**b**) Cr_3C_2-NiCr/TiAlN, (**c**) WC-Co-heating/CrAlN and (**d**) WC-Co-etching/CrAlN. Copyright Elsevier, 2019. Reprinted with permission from Ref. [50]. Copyright Elsevier, 2017. Reprinted with permission from Ref. [62].

However, the porosity of the HVOF-PVD duplex coating is greatly controlled compared to the HVOF coating. It means that the coverage of the PVD coating significantly improves the surface density of the HVOF coating. It is worth mentioning that the particles and pits on the surface of the duplex coating are less prevalent than on the HVOF coating but still more so than on the PVD coating. Pougoum et al. [44] also reported that the surface of the duplex coating had a small portion of clearly visible defects. In the PVD process, the formation of defects is not only related to the deposition process but in many cases mainly originates from irregularities of the substrate, such as large particles and pits [66–69]. The HVOF coating with higher porosity can be regarded as a substrate for the PVD coating in the duplex coating system. Therefore, the PVD top layer will have a certain number of growth defects due to the irregularity of the HVOF bottom layer. In short, the surface quality of the duplex coating is inferior to the PVD coating but superior to the HVOF coating.

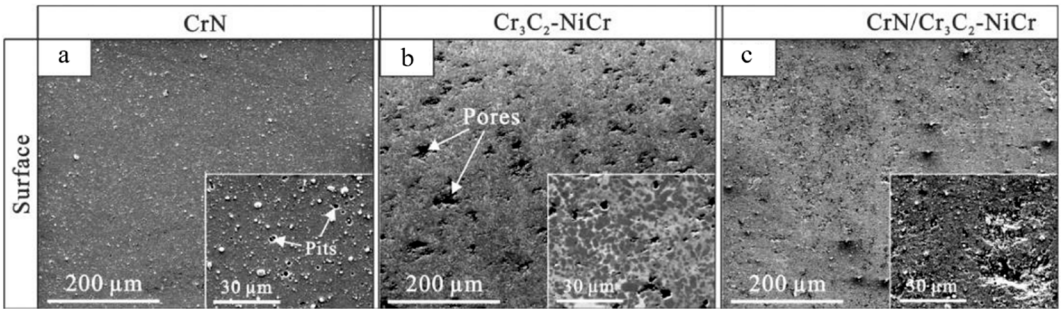

Figure 5. Surface SEM images of (**a**) PVD CrN coating, (**b**) HVOF Cr_3C_2-NiCr coating, and (**c**) HVOF-PVD CrN/Cr_3C_2-NiCr duplex coating. Reprinted with permission from Ref. [55]. Copyright Elsevier, 2019.

3. Properties of Duplex Coatings

3.1. Mechanical Properties

The mechanical properties of the duplex coating are primarily determined by the PVD top layer before it delaminates/flakes off. Therefore, to prevent premature failure of the brittle PVD coatings under high contact stress states, the stress distribution and load-bearing capacity of duplex coatings are particularly essential. In duplex coating designs, the HVOF coating acts as an intermediate layer between the soft substrate and the brittle PVD coating, which typically lies in between in terms of hardness and modulus. It can provide an effective transition and support for the PVD top layer and soft substrate. As a result, the plastic deformation of the substrate due to stress concentration can be avoided when heavy loads are applied, thereby significantly improving the load-bearing capacity of the duplex coating. The contact stress distribution of the material can be visualized from the von Mises stress contour plot obtained through finite element simulations. The von Mises stress distributions of PVD (AlCrN) coating and HVOF-PVD (Cr_3C_2-NiCr/AlCrN) duplex coating are shown in Figure 6 [56]. Here, a simulated load of 15 N is applied to the coating surface.

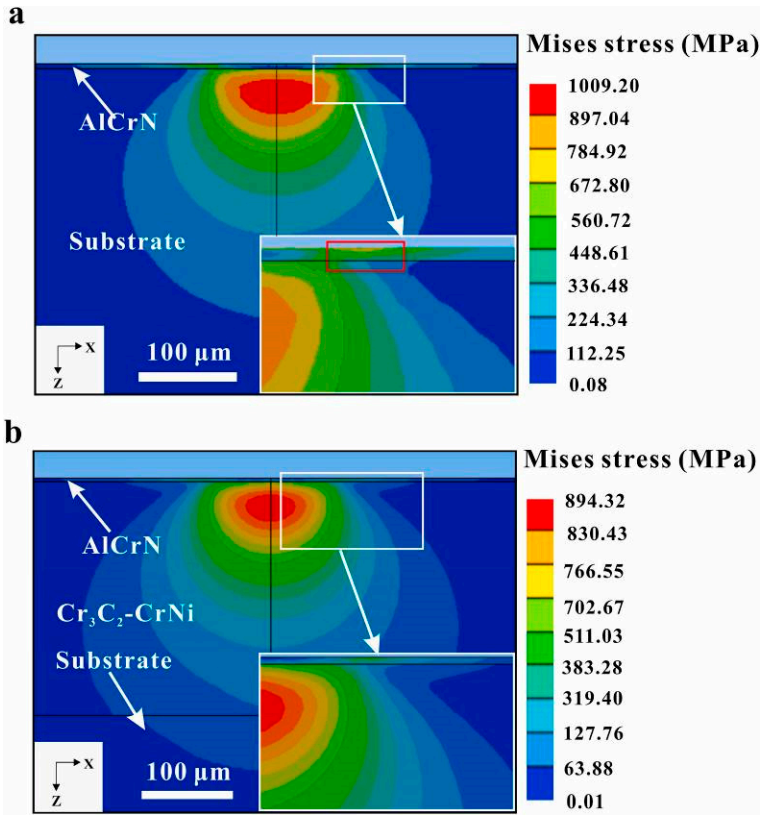

Figure 6. Mises stress distribution of (**a**) PVD coating and (**b**) HVOF-PVD duplex coating. Reprinted with permission from Ref. [56]. Copyright Elsevier, 2022.

For the PVD coating (Figure 6a), the stress concentration region is mainly at the interface of the coating and the substrate. Soft substrates are prone to plastic deformation under high contact stress conditions, which in turn leads to spalling failure of brittle PVD coatings. However, in the duplex coating (Figure 6b), the stress concentration region is confined to the thick and hard HVOF interlayer. Thus, the substrate only bears weak contact stress. In this case, the PVD top layer will not fail rapidly due to the plastic deformation of the substrate. Li et al. [57] investigated the load-bearing capacity of duplex coatings by Vickers indentation and scratching. They studied the effect of different HVOF (Cr_3C_2-NiCr) interlayer thicknesses on the load-bearing capacity of duplex coatings. As shown in Figure 7a, the average indentation diagonal size of the PVD coating is the largest (52.5 μm) when there is no HVOF interlayer. It indicates that soft alloy substrates have difficulty in providing sufficient support for PVD coatings to withstand heavy loads [70]. With the addition of the HVOF interlayer, the load-bearing capacity of the PVD top layer is significantly enhanced.

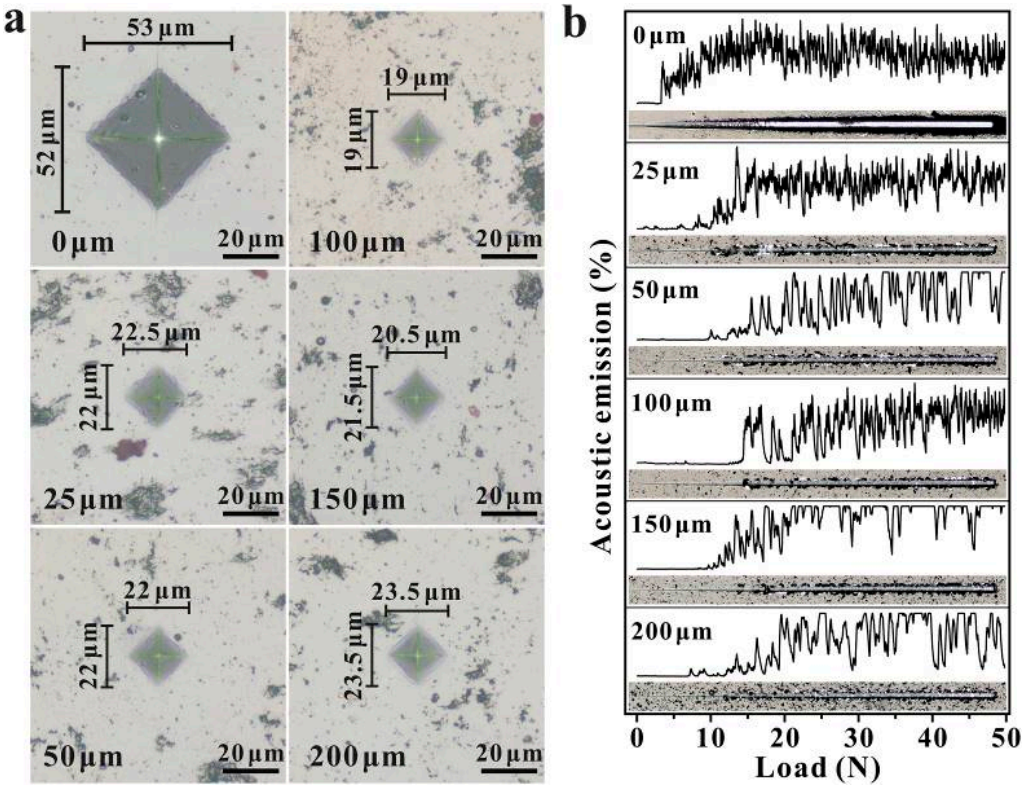

Figure 7. Optical morphology of (**a**) Vickers indentation and (**b**) scratches of the PVD coating and HVOF-PVD duplex coatings. Reprinted with permission from Ref. [57]. Copyright Elsevier, 2022.

It can be understood that the HVOF interlayer provides effective support for the PVD top layer. In addition, the scratch test results (Figure 7b) also show that the HVOF interlayer can significantly improve the interfacial bond strength of the PVD coating. In conclusion, the dual-phase coating design greatly eliminates the stress concentration at the interface between the PVD coating and the soft substrate, effectively inhibiting the plastic deformation of the substrate under heavy load, thereby significantly improving the load-bearing capacity of the PVD coating [71]. Incidentally, once the thickness of the HVOF interlayer covers the stress concentration region, its thickness value has little effect on the load-bearing capacity of the PVD coating. This point can be concluded from the simulation and experimental results of Zheng and Li et al. [56,57].

3.2. Tribological Performance

Tribological properties consist of antifriction and wear resistance, respectively. The low coefficient of friction and wear rate signifies excellent antifriction and wear resistance [72–74]. Initially, the HVOF interlayer was introduced between the PVD top layer and the soft substrate to avoid delamination/collapse of the brittle PVD coating due to the "egg-shell effect" under repeated heavy loading. Therefore, it is not difficult to understand that the wear resistance of the HVOF-PVD duplex coating is significantly improved compared to the PVD single layer. However, the surface roughness of the duplex coating is higher than that of the PVD coating [55]. As a result, the frictional resistance is greater during the sliding process, causing an increase in the coefficient of friction. In short, compared with PVD coating, HVOF-PVD duplex coating has superior wear resistance, but the antifriction is somewhat reduced. The friction coefficients of PVD coating and HVOF-PVD duplex coating on 304 stainless steel are recorded in Figure 8 [51]. It can be seen that both CrN-based and DLC-based duplex coatings have comparable coefficients of friction to the respective PVD single layer. That is to say, the presence of the HVOF interlayer seems to be less important for the antifriction properties of PVD coatings. It has been reported that the HVOF interlayer adversely affects the antifriction performance of the PVD top layer [57]. As shown in Figure 9 [57], it can be found that the friction coefficient of the PVD monolayer is consistently lower and less fluctuating than that of the duplex coating. This can be explained by the surface quality of the coating. As mentioned in Section 2, the surface roughness of the HVOF-PVD duplex coating is greater than that of the PVD monolayer due to the growth defects during the physical vapor deposition [55,58,66], and the rough surface will inevitably cause greater frictional resistance. Therefore, during the friction process, the friction coefficient of the duplex coating is higher than that of the PVD monolayer.

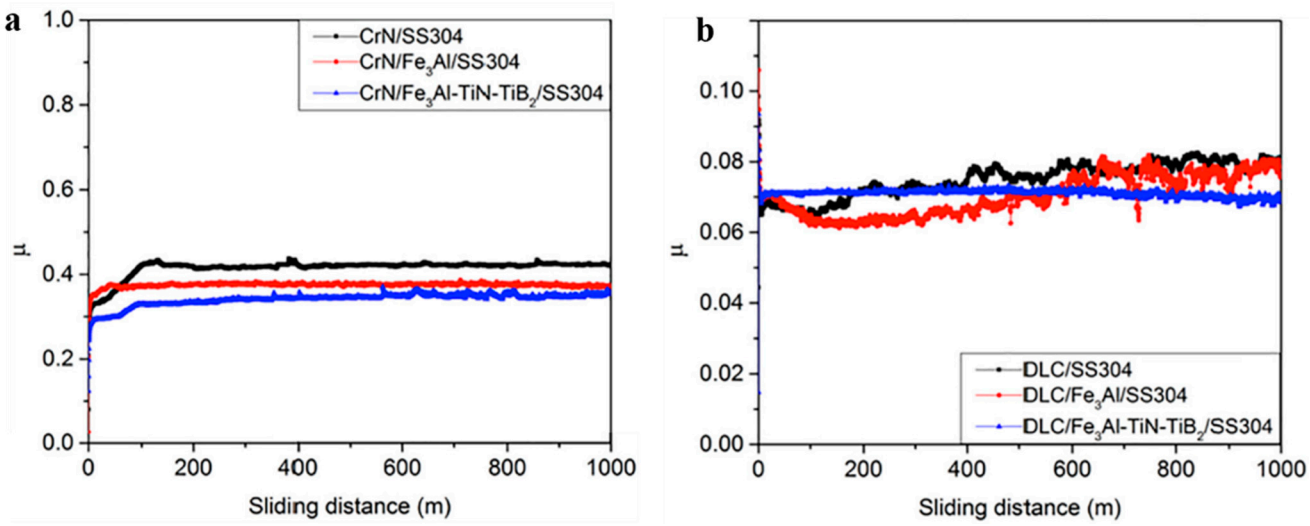

Figure 8. The COF of (**a**) CrN-based and (**b**) DLC-based PVD coating and HVOF-PVD duplex coating on 304 stainless steel. Reprinted with permission from Ref. [51]. Copyright Elsevier, 2018.

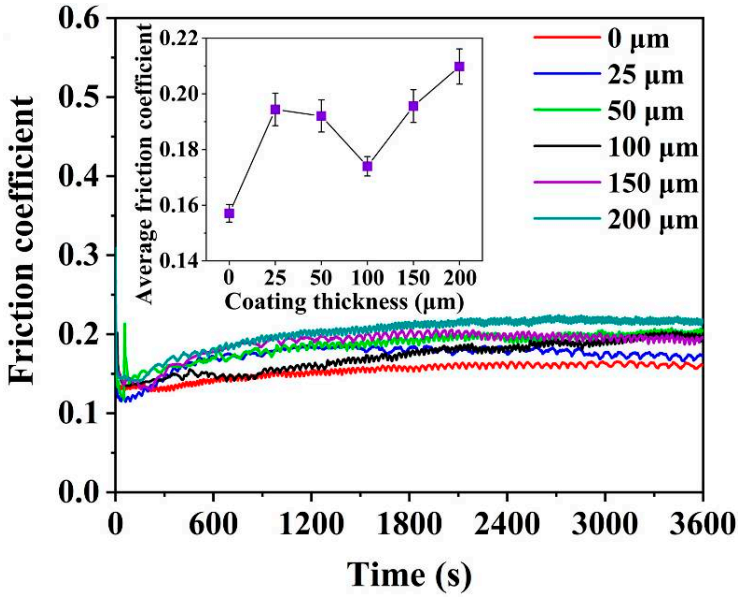

Figure 9. The COF of HVOF-PVD duplex coatings with different HVOF interlayer thicknesses. Reprinted with permission from Ref. [57]. Copyright Elsevier, 2022.

In addition to antifriction, the wear resistance of the duplex coating is also worthy of attention. Figure 10 reports SEM images of the wear tracks of PVD coating and HVOF-PVD duplex coating on Ti6Al4V [61]. It can be observed that the PVD coating (Figure 10a) has undergone catastrophic delamination, and the substrate is visibly grooved under shear with very severe material loss.

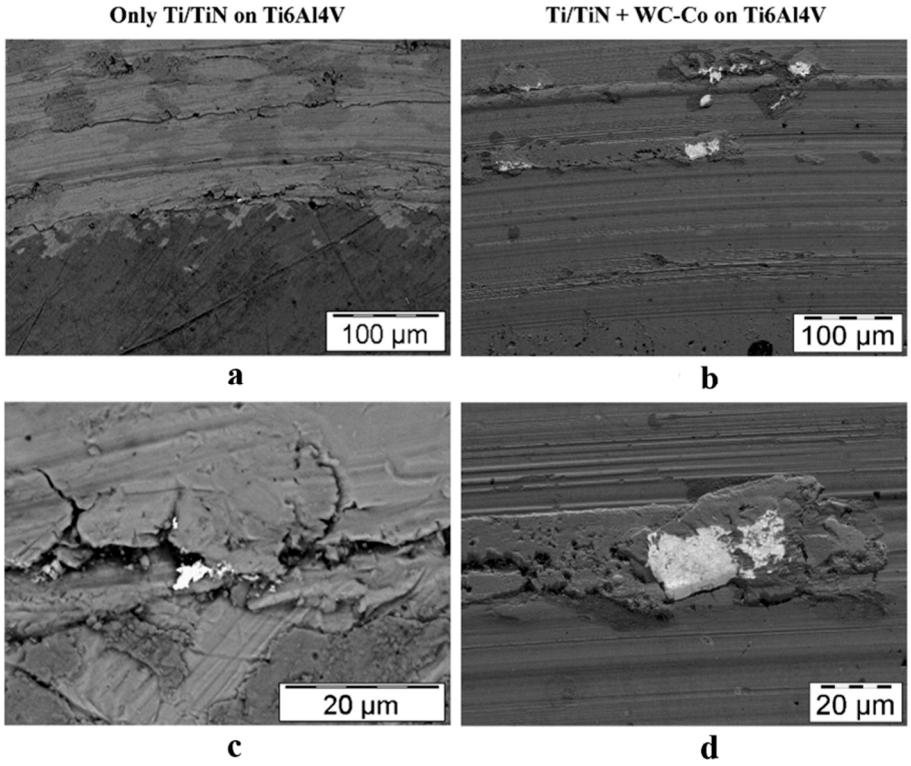

Figure 10. The surface wear track morphology of (**a**,**c**) PVD coating and (**b**,**d**) HVOF-PVD duplex coating on Ti6Al4V substrate. Reprinted with permission from Ref. [61]. Copyright Elsevier, 2008.

While under the same test parameters, the PVD coating in the HVOF-PVD duplex coating (Figure 10b) was not severely delaminated, which only showed deep furrows and

small separations under shear action. It is not difficult to find that the wear resistance of the duplex coating has made a qualitative leap after introducing the HVOF interlayer between the soft substrate and the PVD coating. It can be attributed to the successful transfer of surface contact stresses and improved adhesion in the duplex coating system [53]. It should be further pointed out that the hardness and thickness of the HVOF interlayer will also affect the wear resistance of the duplex coating to a certain extent [51,57]. However, the impact of these factors appears to be negligible.

3.3. Corrosion Behavior

The surface of the HVOF coating is covered with a specific PVD coating, which can enhance its corrosion resistance, including chemical and electrochemical corrosion [44,45,75]. Generally, HVOF coatings present more intrinsic defects, such as pores and cracks, which provide more corrosion channels for corrosive media (Cl^-). In contrast, PVD coatings are dense and virtually defect free. Therefore, the PVD top layer in the duplex coating system can effectively inhibit the corrosive medium Cl^- from entering the interior to penetrate the passivation film (oxide film), thereby delaying the swelling, flaking, and pitting formation of the passivation film. In turn, the corrosion resistance of the HVOF coating is substantially improved. As is well known, the electrochemical corrosion behavior of coatings can be quantitatively evaluated by the potentiodynamic polarization (PDP) and electrochemical impedance spectroscopy (EIS) provided by electrochemical workstations [76,77]. Monticelli et al. [75] investigated the electrochemical corrosion behavior of the HVOF coating and HVOF-PVD duplex coating on steel substrates in a 3.5% NaCl solution. The PDP curves of all specimens are shown in Figure 11a. It can be visually observed that the corrosion resistance of the coated samples is better than that of the steel substrate. To further determine the differences in corrosion behavior of the coated samples, Figure 11b presents the corrosion current densities of all coated samples obtained by Tafel fitting. It can be seen that the current densities of both HVOF-PVD duplex coatings are lower than the respective HVOF coatings. This means that the PVD coating coverage further enhances the corrosion resistance of the HVOF coating. The presence of the coating greatly enhances the resistance of the sample to aggressive ions (Cl^-) [78]. Therefore, it is easy to understand that the corrosion resistance of the coated samples is superior to that of the steel substrate.

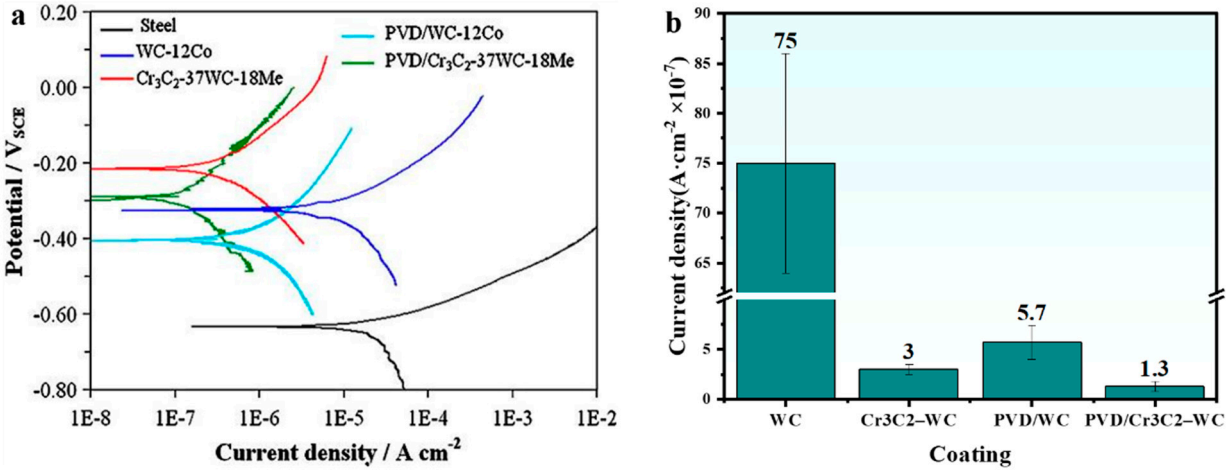

Figure 11. (**a**) Polarization curves and (**b**) corrosion current density of the steel substrate and coating samples in 3.5% NaCl solution. Reprinted with permission from Ref. [75]. Copyright Elsevier, 2010.

However, HVOF coatings have relatively more pores and microcracks, which provide channels for the penetration/diffusion of corrosive media. It will adversely affect the corrosion resistance of the HVOF coating. In this case, the dense PVD coating on the

HVOF coating can serve to seal the pores and block/extend the corrosion channels. Therefore, the PVD coating can be regarded as a strong barrier layer, further preventing the corrosion attack of Cl^- on the HVOF coating and even the substrate. It is the major reason for the superior corrosion resistance of HVOF-PVD duplex coating compared to HVOF coating. As mentioned earlier, EIS is also an important tool to evaluate the electrochemical behavior of coatings. The EIS patterns of the HVOF(Fe3Al) coating and the HVOF-PVD duplex coating are shown in Figure 12 [44]. It can be seen from the Bode plot (Figure 12a) that the phase angles of both HVOF-PVD duplex coatings are always above the HVOF coating. Moreover, the impedance modulus value of the duplex coating is also much higher than that of the HVOF coating. It is further observed from the Nyquist plot (Figure 12b) that the capacitive arc radius of the two HVOF-PVD duplex coatings is significantly larger than that of the HVOF coating. These results indicate that the HVOF-PVD duplex coating plays a more prominent role in hindering the penetration of the corrosion solution than the HVOF coating [79,80]. It is worth mentioning that DLC-covered HVOF coating has a phase angle closer to 90°, a higher impedance modulus, and a larger capacitive arc resistance radius compared to CrN. This indicates that the chemically inert DLC can improve the corrosion resistance of HVOF coatings more significantly than CrN [81]. In short, the corrosion resistance of HVOF-PVD duplex coating is distinctly better than that of HVOF coating, and it is closely related to the type of PVD coating.

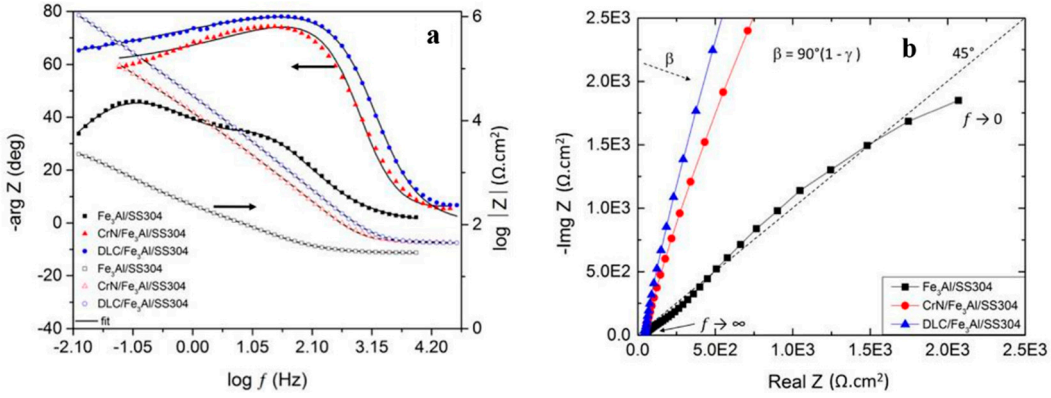

Figure 12. (**a**) Bode and (**b**) Nyquist plots of the Fe3Al, CrN/Fe3Al/SS304 and DLC/Fe3Al/SS304 coatings. Reprinted with permission from Ref. [44]. Copyright Elsevier, 2019.

In addition to electrochemical corrosion, chemical corrosion is also another common corrosion phenomenon that produces loss and damage to materials [82,83]. Tang et al. [45] studied the hot corrosion behavior of HVOF (Cr_3C_2-NiCr) coatings and HVOF-PVD (Cr_3C_2-NiCr/CrN) duplex coatings in mixed salts at 550 °C.

The cross-sectional morphology and element distribution of the HVOF coating and HVOF-PVD duplex coating after hot corrosion for 50 h are shown in Figure 13a,b, respectively. It can be seen that the oxide layer of the HVOF coating exhibits a dark-scale structure with a large number of voids inside. Moreover, the thickness of the oxide layer reaches 13 μm (elemental distribution of oxygen in EDX scan results). In contrast, the oxidation erosion of HVOF-PVD duplex coatings is very restricted. The PVD coating remains relatively intact after hot corrosion, and the thin oxide layer (~1.3 μm) still maintains a dense structure. However, due to the growth defect of the PVD coating [66], localized corrosion occurred in the regions that were not completely covered by the HVOF coating. Based on the above phenomena, it can be known that the coverage of the PVD coating dramatically improves the chemical corrosion resistance of the HVOF coating. This is due to the high number of defects in the HVOF coating, which allows the corrosive medium (Cl^-) to easily enter the interior of the coating. The extremely penetrating Cl^- breaks through the oxide film and triggers oxidation expansion of the inner layer, which in turn causes cracking and flaking [45,84–86]. For comparison, since the duplex coating

has a very dense PVD top layer, it is difficult for the corrosive medium to enter the interior of the coating to attack and destroy. Therefore, under the protection of PVD coating, the HVOF-PVD duplex coating exhibits outstanding hot corrosion resistance.

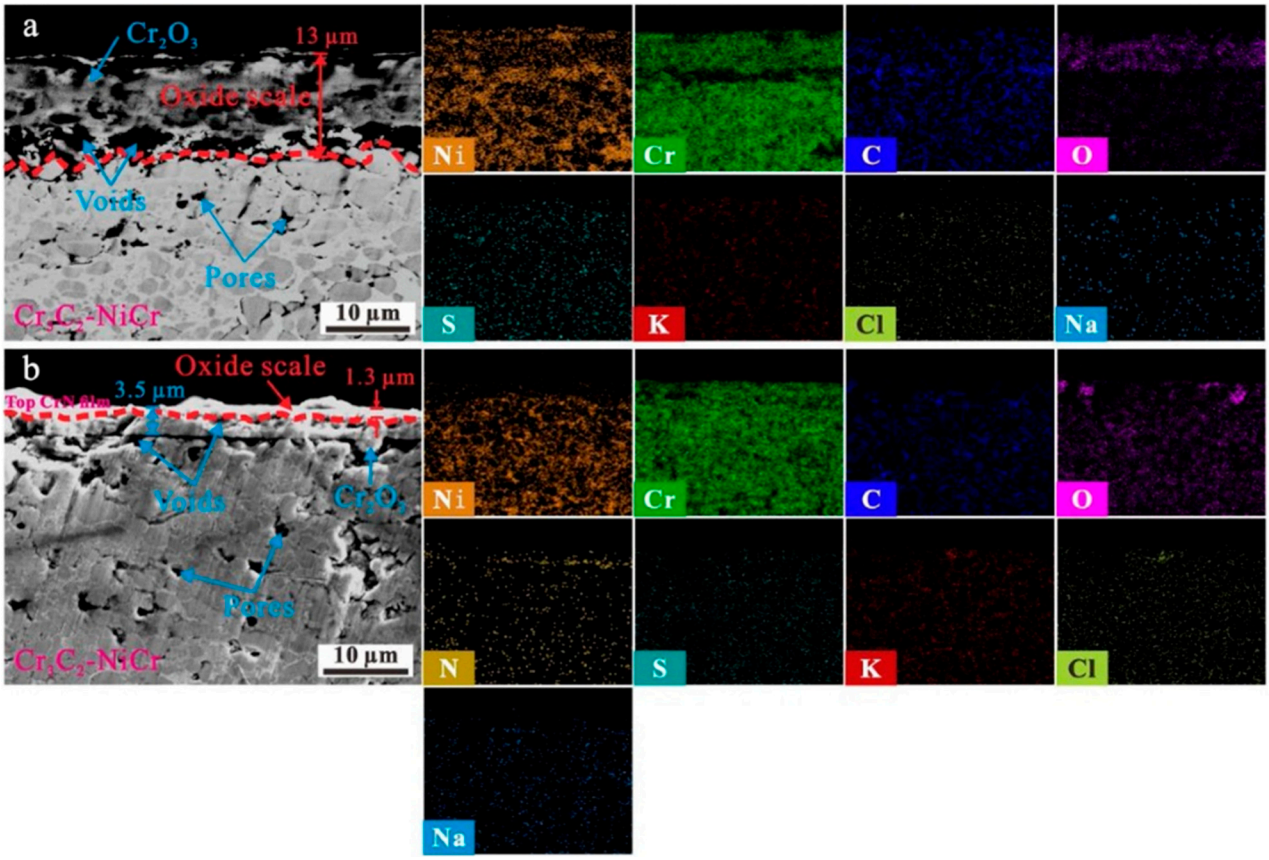

Figure 13. Cross-sectional micrographs and elemental distribution of (**a**) the HVOF coating and (**b**) the HVOF-PVD duplex coating after hot corrosion. Reprinted with permission from Ref. [45]. Copyright Elsevier, 2020.

Finally, the structural characteristics and properties of the duplex protective coatings were summarized in order to obtain a more intuitive overview. The statistical results are listed in Table 1.

Table 1. Performance summary of PVD, HVOF and HVOF-PVD coatings according to the literature in Section 3.

Coating	Dense	Load-Bearing	Anti-Friction	Wear Resistance	Electro-Chemical	Oxidation
PVD	★★★	★	★★★	★	★★★	/
HVOF	★	/	★	/	★	★
HVOF-PVD	★★	★★★	★★	★★★	★★★	★★★

It should be pointed out that since some properties such as denseness and load carrying capacity are difficult to quantify, we used "★" for evaluation, with more "★" meaning better performance. In addition, the specific content of the duplex coating structure and performance is described in detail in Section 3, so it will not be repeated here.

4. Conclusions and Outlook

In this work, we systematically review the microstructure and properties of a high-velocity oxygen-fuel coupled physical vapor deposition (HVOF-PVD) duplex coating

system. Specifically, the morphology (surface and cross-section) of the HVOF-PVD duplex coating and its mechanical (stress and load-bearing capacity), tribological (wear and lubrication), and corrosion (chemical and electrochemical) behavior are described and discussed for surface protective concern (Figure 14). The duplex coating involves a combination of a thick, hard HVOF bottom layer and a thin, hard yet tough PVD top layer. The hardness and modulus of the HVOF coating are between those of the soft substrate and the hard PVD coating, which thereafter provides a smooth transition and effective support between them. As a result, the HVOF interlayer can eliminate the plastic deformation of the substrate due to stress concentration under heavy load, effectively avoiding the "egg-shell effect". As expected, the duplex coating system would provide excellent load-bearing capacity. In terms of tribology, the wear resistance of the HVOF-PVD duplex coating is significantly improved compared to that of PVD monolayer coating. As previously mentioned, due to the supporting effect of the HVOF interlayer, the PVD coating will not undergo catastrophic delamination/flaking, but merely be removed by shearing during the load sliding process. Therefore, duplex coatings favor a longer service life as a protective layer compared to the PVD coatings.

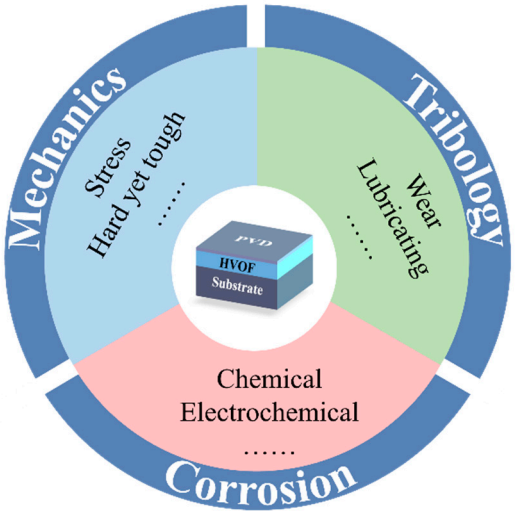

Figure 14. Properties of HVOF-PVD duplex coating, including mechanics, tribology, and corrosion.

However, the roughness of the HVOF coating is higher compared to the soft substrate, which causes the PVD coating grown on the HVOF interlayer to be rougher than that grown on the substrate. Thus, the HVOF-PVD duplex coating is subjected to greater frictional resistance during the sliding process than the PVD coating, resulting in an elevated friction coefficient. It can be summarized that the HVOF interlayer significantly improves the wear resistance of the duplex coating but reduces its antifriction. In terms of corrosion, PVD coatings can significantly enhance the corrosion resistance of duplex coatings, regardless of chemical or electrochemical corrosion. It is because the dense PVD top layer can be considered as a barrier to inhibit the corrosive medium from penetrating/attacking the HVOF coating, thus enhancing the corrosion resistance of the duplex coating system. Therefore, the corrosion resistance of the duplex coating substantially depends on the PVD coating, and the HVOF coating may play a negative role. Finally, research on HVOF-PVD duplex coatings has made some progress. However, there are still several points to ponder in terms of subsequent scientific research and industrial applications:

(a) Rational design and construction of duplex coatings. The comprehensive performance of duplex coatings is not completely superior to that of single coatings. For instance, the introduction of the HVOF interlayer will increase the surface roughness of the PVD coating, which is detrimental to its antifriction properties. In addition, compared to PVD coatings, HVOF coatings with more defects are not beneficial to the corrosion

resistance of duplex coatings. In fact, for PVD coatings, when the load-bearing capacity of the entire film-based system meets the actual working conditions (low/no load case), the design of a duplex coating is not necessary. On the other hand, for thick HVOF coatings, the coverage of thin PVD coatings acts as the "icing on the cake". It means that the protection efficiency of the coating is still strongly dependent on the HVOF coating rather than the PVD coating. In short, a reasonable duplex coating system should be constructed based on the actual application conditions of the material, and whether such a design is required.

(b) Challenges for industrial applications. As we know, HVOF coatings have been widely used for various shapes and sizes of industrial components, such as bridges and offshore platforms. However, for the surface protection of large structural parts, PVD coating is difficult to achieve. On the other hand, small precision parts require high surface quality of the coating, which is a major challenge for the polishing of HVOF coatings. Therefore, dimensional suitability and smooth surface are the bottlenecks for industrial applications of HVOF-PVD duplex coatings.

(c) The wide variety of duplex coatings makes standardization difficult. Both HVOF and PVD coatings are flexible in their option for raw materials. As a result, the combination of HVOF-PVD duplex coating is ever changing. In the future, it will be necessary to perform structural design and performance prediction of duplex coatings by simulation calculations to simplify the experimental process. It will greatly contribute to the development of duplex coatings.

Author Contributions: Conceptualization, Y.Z. and Q.W.; methodology, Q.W. and P.G.; investigation, Y.Z.; data curation, Y.Z.; writing—original draft preparation, Y.Z.; writing—review and editing, C.S.R., A.W.; supervision, A.W.; funding acquisition, A.W. All authors have read and agreed to the published version of the manuscript.

Funding: This research was funded by National Science Fund for Distinguished Young Scholars of China (52025014), A-class pilot of the Chinese Academy of Sciences (XDA22010303), CAS-NST Joint Research Project (174433KYSB20200021), CAS Interdisciplinary Innovation Team (292020000008), K.C. Wong Education Foundation of Chinese Academy of Science (GJTD-2019-13).

Institutional Review Board Statement: Not applicable.

Informed Consent Statement: Not applicable.

Data Availability Statement: Not applicable.

Conflicts of Interest: The authors declare no conflict of interest.

References

1. Tan, J.; Looney, L.; Hashmi, M. Component repair using HVOF thermal spraying. *J. Mater. Process. Technol.* **1999**, *92*, 203–208.
2. Zhang, H.; Wang, X.Y.; Zheng, L.L. Studies of splat morphology and rapid solidification during thermal spraying. *Int. J. Heat Mass Transf.* **2001**, *44*, 4579–4592.
3. Yang, K.; Min, L.; Zhou, K.; Deng, C. Recent Developments in the Research of Splat Formation Process in Thermal Spraying. *J. Mater.* **2012**, *2013*, 1–14.
4. Paredes, R.; Amico, S.; d'Oliveira, A. The effect of roughness and pre-heating of the substrate on the morphology of aluminum coatings deposited by thermal spraying. *Surf. Coat. Technol.* **2006**, *200*, 3049–3055.
5. Niranatlumpong, P.; Koiprasert, H. Phase transformation of NiCrBSi–WC and NiBSi–WC arc sprayed coatings. *Surf. Coat. Technol.* **2011**, *206*, 440–445.
6. Pfender, E. Fundamental studies associated with the plasma spray process. *Surf. Coat. Technol.* **1988**, *34*, 1–14.
7. Wang, J.; Zhang, L.; Sun, B.; Zhou, Y. Study of the Cr3C2–NiCr detonation spray coating. *Surf. Coat. Technol.* **2000**, *130*, 69–73.
8. Stewart, D.; Shipway, P.; McCartney, D. Abrasive wear behavior of conventional and nanocomposite HVOF-sprayed WC–Co coatings. *Wear* **1999**, *225*, 789–798.
9. Wang, Q.; Chen, Z.; Ding, Z. Performance of abrasive wear of WC-12Co coatings sprayed by HVOF. *Tribol. Int.* **2009**, *42*, 1046–1051.
10. Yu, J.; Liu, X.; Yu, Y.; Li, H.; Liu, P.; Huang, K.; Sun, R. Research and Application of High-Velocity Oxygen Fuel Coatings. *Coatings* **2022**, *12*, 828.

11. Brezinova, J.; Guzanová, A.; Draganovska, D.; Maruschak, P.O.; Landová, M. Study of selected proper-ties of thermally sprayed coatings containing WC and WB hard particles. *Acta Mech. Autom*. **2016**, *10*, 296–299.
12. Brezinova, J.; Guzanová, A.; Tkáčová, J.; Brezina, J.; L'achova, K.; Draganovska, D.; Pastorek, F.; Maruschak, P.; Prentkovskis, O. High velocity oxygen liquid-fuel (HVOLF) spraying of WC-based coatings for transport industrial applications. *Metals* **2020**, *10*, 1675.
13. Wang, Q.; Zhang, S.; Cheng, Y.; Xiang, J.; Zhao, X.; Yang, G. Wear and corrosion performance of WC-10Co4Cr coatings deposited by different HVOF and HVAF spraying processes. *Surf. Coat. Technol.* **2013**, *218*, 127–136.
14. Picas, J.; Forn, A.; Matthäus, G. HVOF coatings as an alternative to hard chrome for pistons and valves. *Wear* **2006**, *261*, 477–484.
15. Wielage, B.; Wank, A.; Pokhmurska, H.; Grund, T.; Rupprecht, C.; Reisel, G.; Friesen, E. Development and trends in HVOF spraying technology. *Surf. Coat. Technol.* **2006**, *201*, 2032–2037.
16. Berger, L.-M. Application of hard metals thermal spray coatings. *Int. J. Refract. Met. Hard Mater.* **2015**, *49*, 350–364.
17. Wang, Q.; Luo, S.; Wang, S.; Wang, H.; Ramachandran, C.S. Wear, erosion and corrosion resistance of HVOF-sprayed WC and Cr3C2 based coatings for electrolytic hard chrome replacement. *Int. J. Refract. Met. Hard Mater.* **2019**, *81*, 242–252.
18. Picas, J.; Punset, M.; Baile, M.T.; Martín, E.; Forn, A. Effect of oxygen/fuel ratio on the in-flight particle parameters and properties of HVOF WC-CoCr coatings. *Surf. Coat. Technol.* **2011**, *205*, S364–S368.
19. Roy, M.; Pauschitz, A.; Bernardi, J.; Koch, T.; Franek, F. Microstructure and mechanical properties of HVOF sprayed nanocrystalline Cr3C2-25 (Ni20Cr) coating. *J. Therm. Spray Technol.* **2006**, *15*, 372–381.
20. Zhang, C.; Liu, L.; Chan, K.C.; Chen, Q.; Tang, C.Y. Wear behavior of HVOF-sprayed Fe-based amorphous coatings. *Intermetallics* **2012**, *29*, 80–85.
21. Lovelock, H.L.D.V. Powder/processing/structure relationships in WC-Co thermal spray coatings: A review of the published literature. *J. Therm. Spray Technol.* **1998**, *7*, 357–373.
22. Guilemany, J.M.; Fernández, J.; Delgado, J.; Benedetti, A.V.; Clement, F. Effects of thickness coating on the electrochemical behavior of thermal spray Cr3C2–NiCr coatings. *Surf. Coat. Technol.* **2002**, *153*, 107–113.
23. Huang, B.; Zhang, C.; Zhang, G.; Liao, H. Wear and corrosion resistant performance of thermal-sprayed Fe-based amorphous coatings: A review. *Surf. Coat. Technol.* **2019**, *377*, 124896.
24. Poblano-Salas, C.; Cabral-Miramontes, J.; Gallegos-Melgar, A.; Ruiz-Luna, H.; Aguilar-Escobar, J.; Espinosa-Arbelaez, D.; Espinoza-Beltrán, F.; Trapaga-Martínez, G.; Muñoz-Saldaña, J. Effects of VC additions on the mechanical properties of bimodal WC–Co HVOF thermal sprayed coatings measured by nanoindentation. *Int. J. Refract. Met. Hard Mater.* **2015**, *48*, 167–178.
25. Yin, B.; Liu, G.; Zhou, H.; Chen, J.; Yan, F. Sliding wear behavior of HVOF-sprayed Cr3C2–NiCr/CeO2 composite coatings at elevated temperature up to 800 °C. *Tribol. Lett.* **2010**, *37*, 463–475.
26. Wang, Q.; Zhang, Y.; Ding, X.; Wang, S.; Ramachandran, C.S. Effect of WC grain size and abrasive type on the wear performance of HVOF-sprayed WC-20Cr3C2-7Ni coatings. *Coatings* **2020**, *10*, 660.
27. Li, M.; Christofides, P.D. Modeling, and control of high-velocity oxygen-fuel (HVOF) thermal spray: A tutorial review. *J. Therm. Spray Technol.* **2009**, *18*, 753–768.
28. Baptista, A.; Silva, F.; Porteiro, J.; Míguez, J.; Pinto, G. Sputtering physical vapor deposition (PVD) coatings: A critical review on process improvement and market trend demand. *Coatings* **2018**, *8*, 402.
29. Helmersson, U.; Lattemann, M.; Bohlmark, J.; Ehiasarian, A.; Gudmundsson, J. Ionized physical vapor deposition (IPVD): A review of technology and applications. *Thin Solid Film.* **2006**, *513*, 1–24.
30. Rossnagel, S. Thin film deposition with physical vapor deposition and related technologies. *J. Vac. Sci. Technol. A Vac. Surf. Film.* **2003**, *21*, S74–S87.
31. Mattox, D.M. Physical vapor deposition (PVD) processes. *Met. Finish.* **1995**, *93*, 387–388.
32. Liu, Y.; Guo, P.; He, X.; Li, L.; Wang, A.; Li, H. Developing transparent copper-doped diamond-like carbon films for marine antifouling applications. *Diam. Relat. Mater*. **2016**, *69*, 144–151.
33. Baptista, A.; Silva, F.; Porteiro, J.; Míguez, J.; Pinto, G.; Fernandes, L. On the physical vavaporeposition (PVD): Evolution of magnetron sputtering processes for industrial applications. *Procedia Manuf.* **2018**, *17*, 746–757.
34. Zuo, X.; Zhang, D.; Chen, R.; Ke, P.; Odén, M.; Wang, A. Spectroscopic investigation on the near-substrate plasma characteristics of chromium HiPIMS in low-density discharge mode. *Plasma Sources Sci. Technol.* **2020**, *29*, 015013.
35. Wang, Z.; Kang, H.; Chen, R.; Ke, P.; Wang, A. Enhanced mechanical and tribological properties of V-Al-C coatings via increasing columnar boundaries. *J. Alloys Compd.* **2019**, *781*, 186–195.
36. Shuai, J.; Zuo, X.; Wang, Z.; Guo, P.; Xu, B.; Zhou, J.; Wang, A.; Ke, P. Comparative study on the rack resistance of TiAlN monolithic and Ti/TiAlN multilayer coatings. *Ceram. Int.* **2020**, *46*, 6672–6681.
37. Wang, Z.; Liu, J.; Wang, L.; Li, X.; Ke, P.; Wang, A. Dense, and high-stability Ti2AlN MAX phase coatings prepared by the combined cathodic arc/sputter technique. *Appl. Surf. Sci.* **2017**, *396*, 1435–1442.
38. Ruan, H.; Wang, Z.; Wang, L.; Sun, L.; Peng, H.; Ke, P.; Wang, A. Designed Ti/TiN sub-layers suppressing the crack and erosion of TiAlN coatings. *Surf. Coat. Technol.* **2022**, *438*, 128419.

39. Wang, A.-Y.; Lee, K.-R.; Ahn, J.-P.; Han, J.H. Structure and mechanical properties of W incorporated diamond-like carbon films prepared by a hybrid ion beam deposition technique. *Carbon* **2006**, *44*, 1826–1832.
40. Wang, Z.; Li, X.; Zhou, J.; Liu, P.; Huang, Q.; Ke, P.; Wang, A. Microstructure evolution of V–Al–C coatings synthesized from a V2AlC compound target after vacuum annealing treatment. *J. Alloys Compd.* **2016**, *661*, 476–482.
41. Barshilia, H.C.; Selvakumar, N.; Deepthi, B.; Rajam, K. A comparative study of reactive direct current magnetron sputtered CrAlN and CrN coatings. *Surf. Coat. Technol.* **2006**, *201*, 2193–2201.
42. Hainsworth, S.V.; Soh, W. The effect of the substrate on the mechanical properties of TiN coatings. *Surf. Coat. Technol.* **2003**, *163*, 515–520.
43. Zhao, W.M.; Wang, Y.; Dong, L.X.; Wu, K.Y.; Xue, J. Corrosion mechanism of NiCrBSi coatings deposited by HVOF. *Surf. Coat. Technol.* **2005**, *190*, 293–298.
44. Pougoum, F.; Qian, J.; Martinu, L.; Klemberg-Sapieha, J.; Zhou, Z.; Li, K.Y.; Savoie, S.; Lacasse, R.; Potvin, E.; Schulz, R. Study of corrosion and tribocorrosion of Fe3Al-based duplex PVD/HVOF coatings against alumina in NaCl solution. *Surf. Coat. Technol.* **2019**, *357*, 774–783.
45. Tang, P.; He, D.; Li, W.; Shang, L.; Zhang, G. Achieving superior hot corrosion resistance by PVD/HVOF duplex design. *Corros. Sci.* **2020**, *175*, 108845.
46. Li, X.; Xu, X.; Zhou, Y.; Lee, K.; Wang, A. Insights into friction dependence of carbon nanoparticles as oil-based lubricant additive at amorphous carbon interface. *Carbon* **2019**, *150*, 465–474.
47. Erdemir, A.; Martin, J.M. Superior wear resistance of diamond and DLC coatings. *Curr. Opin. Solid State Mater. Sci.* **2018**, *22*, 243–254.
48. Kong, C.; Guo, P.; Sun, L.; Zhou, Y.; Liang, Y.; Li, X.; Ke, P.; Lee, K.-R.; Wang, A. Tribological mechanism of diamond-like carbon films induced by Ti/Al co-doping. *Surf. Coat. Technol.* **2018**, *342*, 167–177.
49. Dang, N.M.; Lin, W.-Y.; Wang, Z.-Y.; Alidokht, S.A.; Chromik, R.R.; Chen, T.Y.-F.; Lin, M.-T. Mechanical Properties and Residual Stress Measurement of TiN/Ti Duplex Coating Using HiPIMS TiN on Cold Spray Ti. *Coatings* **2022**, *12*, 759.
50. Picas, J.; Menargues, S.; Martin, E.; Colominas, C.; Baile, M. Characterization of duplex coating system (HVOF+ PVD) on light alloy substrates. *Surf. Coat. Technol.* **2017**, *318*, 326–331.
51. Pougoum, F.; Qian, J.; Laberge, M.; Martinu, L.; Klemberg-Sapieha, J.; Zhou, Z.; Li, K.Y.; Savoie, S.; Schulz, R. Investigation of Fe3Al-based PVD/HVOF duplex coatings to protect stainless steel from sliding wear against alumina. *Surf. Coat. Technol.* **2018**, *350*, 699–711.
52. Tillmann, W.; Stangier, D.; Hagen, L.; Schröder, P.; Krabiell, M. Influence of the WC grain size on the properties of PVD/HVOF duplex coatings. *Surf. Coat. Technol.* **2017**, *328*, 326–334.
53. Bemporad, E.; Sebastiani, M.; Casadei, F.; Carassiti, F. Modelling, product, action, and characterization of duplex coatings (HVOF and PVD) on Ti–6Al–4V substrate for specific mechanical applications. *Surf. Coat. Technol.* **2007**, *201*, 7652–7662.
54. Bemporad, E.; Sebastiani, M.; De Felicis, D.; Carassiti, F.; Valle, R.; Casadei, F. Production, and characterization of duplex coatings (HVOF and PVD) on Ti–6Al–4V substrate. *Thin Solid Film.* **2006**, *515*, 186–194.
55. Li, W.; Tang, P.; Shang, L.; He, D.; Wang, L.; Zhang, G.; Jin, K. Tribological behaviors of CrN/Cr3C2-NiCr duplex coating at elevated temperatures. *Surf. Coat. Technol.* **2019**, *378*, 124926.
56. Zheng, W.; He, D.; Li, W.; Shang, L.; Song, Q.; Zhang, G.; Zhai, H.; Cheng, B. AlCrN/Cr3C2–NiCr duplex coating towards high load-bearing and dry sliding antiwear applications. *Ceram. Int.* **2022**, *48*, 18933–18943.
57. Li, W.; Zhao, Y.; He, D.; Song, Q.; Sun, X.; Wang, S.; Zhai, H.; Zheng, W.; Wood, R.J. Optimizing mechanical and tribological properties of DLC/Cr3C2-NiCr duplex coating via tailoring interlayer thickness. *Surf. Coat. Technol.* **2022**, *434*, 128198.
58. Shang, L.; Li, W.; He, D.; Tang, P.; Zhang, G.; Lu, Z. Mechanical and high-temperature tribological properties of Cr3C2-NiCr/TiN duplex coating. *J. Mater. Eng. Perform.* **2020**, *29*, 7207–7220.
59. Chen, W.; Fang, B.; Zhang, D.; Meng, X.; Zhang, S. Thermal stability and mechanical properties of HVOF/PVD duplex ceramic coatings produced by HVOF and cathodic vacuum arc. *Ceram. Int.* **2017**, *43*, 7415–7423.
60. Lima, C.; Cinca, N.; Guilemany, J. Study of the high-temperature oxidation performance of Thermal Barrier Coatings with HVOF sprayed bond coat and incorporating a PVD ceramic interlayer. *Ceram. Int.* **2012**, *38*, 6423–6429.
61. Bemporad, E.; Sebastiani, M.; Staia, M.; Cabrera, E.P. Tribological studies on PVD/HVOF duplex coatings on Ti6Al4V substrate. *Surf. Coat. Technol.* **2008**, *203*, 566-571.
62. Tillmann, W.; Hagen, L.; Stangier, D.; Krabiell, M.; Schröder, P.; Tiller, J.; Krumm, C.; Sternemann, C.; Paulus, M.; Elbers, M. Influence of etching-pretreatment on nano-grained WC-Co surfaces and properties of PVD/HVOF duplex coatings. *Surf. Coat. Technol.* **2019**, *374*, 32–43.
63. Dai, W.; Wu, G.; Wang, A. Preparation, characterization, and properties of Cr-incorporated DLC films on magnesium alloy. *Diamond Relat. Mater.* **2010**, *19*, 1307–1315.
64. Shuai, J.; Zuo, X.; Wang, Z.; Sun, L.; Chen, R.; Wang, L.; Wang, A.; Ke, P. Erosion behavior and failure mechanism of Ti/TiAlN multilayer coatings eroded by silica sand and glass beads. *J. Mater. Sci. Technol.* **2021**, *21*, 12.
65. Wang, Q.; Li, L.; Yang, G.; Zhao, X.; Ding, Z. Influence of heat treatment on the microstructure and performance of high-velocity oxy-fuel sprayed WC–12Co coatings. *Surf. Coat. Technol.* **2012**, *206*, 4000–4010.

66. Panjan, P.; Drnovšek, A.; Gelman, P.; Čekada, M.; Panjan, M. Review of growth defects in thin films prepared by PVD techniques. *Coatings* **2020**, *10*, 447.
67. Panjan, P.; Gselman, P.; Kek-Merl, D.; Čekada, M.; Panjan, M.; Dražić, G.; Bončina, T.; Zupanič, F. Growth defect density in PVD hard coatings prepared by different deposition techniques. *Surf. Coat. Technol.* **2013**, *237*, 349–356.
68. Panjan, P.; Ekada, M.; Panjan, M.; Kek-Merl, D. Growth defects in PVD hard coatings. *Vacuum* **2009**, *84*, 209–214.
69. Liu, Y.; Du, H.; Zuo, X.; Guo, P.; Ke, P. Cr/GLC multilayered coating in the simulated deep-sea environment: Corrosion behavior and growth defect evolution. *Corros. Sci.* **2021**, *188*, 109528.
70. Wänstrand, O.; Larsson, M.; Kassman-Rudolphi, Å. An experimental method for evaluation of the load-carrying capacity of coated aluminum: The influence of coating stiffness, hardness, and thickness. *Surf. Coat. Technol.* **2000**, *127*, 107–113.
71. Chen, W.; Mao, T.; Zhang, B.; Zhang, S.; Meng, X. Designs and preparation of advanced HVOF-PVD duplex coating by a combination of HVOF and arc ion plating. *Surf. Coat. Technol.* **2016**, *304*, 125–133.
72. Hogmark, S.; Jacobson, S.; Larsson, M. Design, and evaluation of tribological coatings. *Wear* **2000**, *246*, 20–33.
73. Donnet, C.; Erdemir, A. Historical developments and new trends in tribological and solid lubricant coatings. *Surf. Coat. Technol.* **2004**, *180*, 76–84.
74. Voevodin, A.A.; O'Neill, J.P.; Zabinski, J.S. Nanocomposite tribological coatings for aerospace applications. *Surf. Coat. Technol.* **1999**, *116–119*, 36–45.
75. Monticelli, C.; Balbo, A.; Zucchi, F. Corrosion and tribocorrosion behavior of cermet and cermet/nanoscale multilayer CrN/NbN coatings. *Surf. Coat. Technol.* **2010**, *204*, 1452–1460.
76. Li, Y.; Qu, L.; Wang, F. The electrochemical corrosion behavior of TiN and (Ti, Al)N coatings in acid and salt solution. *Corros. Sci.* **2003**, *45*, 1367–1381.
77. Duan, H.; Du, K.; Yan, C.; Wang, F. Electrochemical corrosion behavior of composite coatings of sealed MAO film on magnesium alloy AZ91D. *Electrochim. Acta* **2006**, *51*, 2898–2908.
78. Zhang, Y.; Wang, Q.; Chen, G.; Ramachandran, C.S. Mechanical, tribological, and corrosion physiognomies of CNT-Al metal matrix composite (MMC) coatings deposited by cold gas dynamic spray (CGDS) process. *Surf. Coat. Technol.* **2020**, *403*, 126380.
79. Mda, B.; Munk, C.; Ys, C.; Cmk, A.; Akk, D.; Pk, B.; Mm, B.; Pm, D.; Park, B.; Rkg, C. Modification of surface hardness, wear resistance and corrosion resistance of cold spray Al coated AZ31B Mg alloy using cold spray double layered Ta/Ti coating in 3.5wt%NaCl solution. *Corros. Sci.* **2020**, *176*, 109029.
80. Gong, Y.; Geng, J.; Huang, J.; Chen, Z.; Wang, H. Self-healing performance and corrosion resistance of novel CeO2-sealed MAO film on aluminum alloy. *Surf. Coat. Technol.* **2021**, *417*, 127208.
81. Zhao, Y.; Xu, F.; Zhang, D.; Xu, J.; Shi, X.; Sun, S.; Zhao, W.; Gao, C.; Zuo, D. Enhanced tribological and corrosion properties of DLC/CrN multilayer films deposited by HPPMS. *Ceram. Int.* **2022**, *48*, 25569–25577.
82. Santosh, K.; Manoj, K.; Amit, H. Combating hot corrosion of boiler tubes—A study. *Eng. Fail. Anal.* **2018**, *94*, 379–395.
83. Wang, Z.; Ma, G.; Li, Z.; Ruan, H.; Yuan, J.; Wang, L.; Ke, P.; Wang, A. Corrosion mechanism of Ti2AlC MAX phase coatings under the synergistic effects of water vapor and solid NaCl at 600 °C. *Corros. Sci.* **2021**, *192*, 109788.
84. Wang, J.; Li, D.; Shao, T. Hot corrosion and electrochemical behavior of NiCrAlY, NiCoCrAlY and NiCoCrAlYTa coatings in molten NaCl-Na2SO4 at 800 °C. *Surf. Coat. Technol.* **2022**, *440*, 128503.
85. Verdian, M.M.; Raeissi, K.; Salehi, M. The Corrosion performance of HVOF and APS thermally sprayed NiTi intermetallic coatings in 3.5% NaCl solution. *Corros. Sci.* **2010**, *52*, 1052–1059.
86. Liu, C.; Bi, Q.; Matthews, A. EIS comparison on corrosion performance of PVD TiN and CrN coated mild steel in 0.5 N NaCl aqueous solution. *Corros. Sci.* **2001**, *43*, 1953–1961.